Effect of Ligands within Vanadium Complex Encapsulated in Y Zeolite Catalysts on Liquid-phase Benzene Oxidation

Tani, Shotaro
Ichihashi, Yuichi

(Citation)
Journal of the Japan Petroleum Institute,67(2):80-88

(Issue Date)
2024-03-01

(Resource Type)
journal article

(Version)
Version of Record

[Regular Paper]

Effect of Ligands within Vanadium Complex Encapsulated in Y Zeolite Catalysts on Liquid-phase Benzene Oxidation

Shotaro TANI[†1)] and Yuichi ICHIHASHI*[†1),†2)]

[†1)] Dept. of Chemical Science and Engineering, Graduate School of Engineering, Kobe University, Rokkodai, Nada-ku, Kobe 657-8501, JAPAN
[†2)] Research Center for Membrane and Film Technology, Graduate School of Engineering, Kobe University, Rokkodai, Nada-ku, Kobe 657-8501, JAPAN

(Received September 26, 2023)

Vanadium-loaded catalysts used in direct liquid-phase oxidation of benzene have low reusability attributable to the elution of V species into the reaction solution. Herein, V complexes were encapsulated in Y zeolite to prevent the elution of V species in the catalyst used for phenol formation during the direct oxidation of benzene in the liquid phase. V complex catalysts encapsulated in Y zeolite were prepared by mixing Y zeolite loaded with V species using solutions containing different ligands. Using acetic acid as the solvent improved the reusability of the encapsulated V complex catalyst. The catalytic activity of the V complex catalyst for phenol formation was influenced by the ligand effect. Density functional theory (DFT) calculations indicated that the type of ligand also affected the energy gap between V^{3+} and V^{4+}, which is directly related to phenol formation in the present reaction. DFT calculations were further used to identify the mechanism for the liquid-phase oxidation of benzene.

Keywords
Benzene oxidation, Phenol synthesis, Vanadium encapsulated catalyst, Y zeolite, Partial oxidation

1. Introduction

Selective catalytic oxidation reactions of hydrocarbons have significant industrial applications, such as the production of alcohols, aldehydes, ketones, carboxylic acids, and epoxides[1)~6)]. Consequently, an economical, low-energy, and green catalytic process for these industrial products is sought after and has been actively researched.

Phenol is an important chemical with diverse applications in resins, fibers, and medicines. The current industrial cumene production process has a 5 % yield with 95 % selectivity for phenol and produces an equimolecular amount of acetone as a byproduct. The cumene process is widely used in chemical industries because of its high selectivity and demand for acetone. However, this high-energy method requires a three-step reaction and a distillation process to separate the products and reactants. Therefore, the direct oxidation of benzene is an economically desirable process for phenol production without forming byproducts. Numerous researchers have investigated the selective oxidation of benzene in the one-step synthesis of phenols. In particular, Panov et al.[7),8)], Yoo et al.[9)], Jia et al.[10)], and Horváth et al.[11)] reported the gas-phase oxidation of benzene to phenol over Fe-loaded catalysts under an N_2O atmosphere. They achieved a yield of 4.2 % with $>$95 % selectivity for the gas-phase hydroxylation of benzene using a mixture of air and ammonia over copper-based phosphate catalysts. A few researchers have also reported the liquid-phase hydroxylation of benzene using TEMPO[12)] or hydrogen peroxide[13)~17)]. With increasing demand for environment friendly and cost-effective chemistry, there is a growing demand for the catalytic oxidation of benzene employing green oxidants, such as O_2 with few additives[18)~23)]. Although typical oxidants, such as N_2O, give high yields of products they are too expensive for practical purposes. Therefore, a one-step synthesis of phenol from benzene without additives is desirable for industrial applications.

We have previously investigated the direct oxidation of benzene in the liquid phase using V-loaded catalysts and molecular O_2[24),25)]. However, the used catalysts had a low reusability, which was attributed to the elution of V species into the reaction solution. We explored a method that prevents V species from eluting

DOI: doi.org/10.1627/jpi.67.80
* To whom correspondence should be addressed.
* E-mail: ichiy@kobe-u.ac.jp

into the reaction solutions by preparing V complex catalysts in Y zeolite within the zeolite pores. This approach offers several advantages, including the transformation of the homogeneous catalyst into a heterogeneous one and enhanced catalyst reusability. The interaction between the supported zeolite and the complex suppresses steric hindrance and elution of the active species. When the V-complex-encapsulated Y zeolite catalyst was used for the liquid-phase oxidation of benzene, the catalyst's reusability was improved. Furthermore, the catalytic activity differed depending on the coordination of the encapsulated complex. In this study, we prepared a V-complex-encapsulated Y zeolite catalyst using p-substituted benzoic acid as a ligand and evaluated its activity for the one-step synthesis of phenol through the direct oxidation of benzene. The effects of the ligands on reaction activity and the mechanism of this reaction were also investigated. Moreover, we attempted to elucidate the benzene liquid-phase oxidation reaction mechanism using quantum chemical calculations and examined the oxidation process in detail.

2. Experimental

2. 1. Material

Benzene, ascorbic acid, acetic acid, sucrose, sulfuric acid, glucose, fructose, potassium permanganate, and aqueous solution of 30 %w/w hydrogen peroxide (Nacalai Tesque, Inc., guaranteed reagent) were used as received without further purification.

2. 2. Preparation of Catalyst

2. 2. 1. Preparation of V Complex Catalysts Encapsulated in Y Zeolite

V complex catalysts encapsulated in Y zeolite were prepared through ion exchange with H-Y zeolite. Ion exchange was performed by adding H-Y zeolite (Zeolyst, $SiO_2/Al_2O_3 = 5$, 3 g) to an aqueous vanadium (IV) oxide sulfate solution and leaving it at 353 K for 48 h. The mixture was then filtered, washed, and dried overnight at 393 K. The oxovanadium ion was anchored on the Y zeolite and designated as V-Y. V-Y and various ligands were dispersed in methanol, and the mixture was refluxed with stirring at 333 K for 20 h, filtered, and washed with methanol. The obtained solid was refluxed with continuous stirring at 333 K for 5 h in methanol, filtered, washed with methanol, and dried at 393 K for 24 h to obtain the V complex catalyst encapsulated in Y zeolite. Benzoic acid (BA), *p*-aminobenzoic acid (ABA), *p*-hydroxybenzoic acid (HBA), *p*-methylbenzoic acid (MBA), *p*-chlorobenzoic acid (CBA), and *p*-nitrobenzoic acid (NBA) were used as ligands.

2. 2. 2. Preparation of V-loaded Y Zeolite Catalyst

The V-loaded Y zeolite catalyst was prepared by stirring the H-Y zeolite and vanadium oxide sulfate in methanol, evaporating to dryness in a hot water bath, and drying overnight at 393 K. The obtained solid was denoted as V/H-Y.

2. 2. 3. Preparation of Ligand-loaded Y Zeolite Catalysts

Ligand-loaded Y zeolite catalysts were prepared by stirring the H-Y zeolite and various ligands in methanol, evaporating to dryness at 333 K in a hot water bath, and drying overnight at 393 K. The obtained solid was denoted as PA/H-Y.

2. 3. Catalyst Evaluation

2. 3. 1. Liquid-phase Oxidation of Benzene

A 0.5 mL sample of benzene (5.6 mmol), catalyst (0.1 g), sucrose (0.4 mmol), and 5 mL of an aqueous acetic acid solution (20 vol%) were added to a stainless steel pressured reactor (Taiatsu Glass Co.; inner diameter, 1.7 cm; height, 11.2 cm)[23]. Oxidation was conducted for 20 h under stirring using a magnetic stirrer at 353 K in an O_2 atmosphere of 0.4 MPa. After oxidation, 5 mL of 2-propanol containing toluene (0.5 vol%), which was confirmed to be unchanged during the after-treatment, was added to the reaction mixture as an internal standard. After the centrifugal separation of the solid catalyst, the reaction products were analyzed using HPLC (JASCO Corp.). The used catalysts were washed thrice with acetone, dried overnight at 393 K, and recycled for the next reaction.

2. 3. 2. Using Hydrogen Peroxide Reaction Performed under the Following Condition

A 0.5 mL sample of benzene (5.6 mmol), catalyst (0.1 g), sucrose (0.4 mmol), and 1 mL of an aqueous hydrogen peroxide solution (30 wt%) were added into a stainless-steel pressured reactor (Taiatsu Glass Co.; inner diameter, 1.7 cm; height, 11.2 cm). The reaction mixture was oxidized for 90 min under stirring using a magnetic stirrer at 353 K under an N_2 atmosphere of 0.4 MPa.

2. 3. 3. Determination of the Amount of Hydrogen Peroxide Generated

Catalyst (0.1 g), sucrose (0.4 mmol), and 5 mL of an aqueous acetic acid solution (20 vol%) were added to a stainless-steel pressured reactor (Taiatsu Glass Co.; inner diameter, 1.7 cm; height, 11.2 cm). Oxidation was conducted for 20 h under stirring using a magnetic stirrer at 353 K in an O_2 atmosphere of 0.4 MPa. Sulfuric acid (1 mL) was added to 5.5 mL of the solution after reaction, and the volume was made up to 30 mL with distilled water. Titration was then carried out using 0.02 mol/L potassium permanganate.

2. 4. Characterization

X-ray diffraction (XRD) patterns of fresh and used catalysts were collected at 298 K using a Rigaku RINT 2000 XRD instrument with a Cu Kα source. Samples were step-scanned from $2\theta = 5.0°$ to 60.0°, with 0.02° steps and 1.0 scanned counts.

Nitrogen physisorption measurements were per-

Table 1 Chemical Composition and Physical Properties of Catalysts

Catalyst	V loading [mmol/g]	BET surface area [m^2/g]
H-Y (Si/Al = 2.5)	-	702
V-Y	0.89	343
V(BA)-Y	0.70	405
V(ABA)-Y	0.59	455
V(HBA)-Y	0.57	463
V(MBA)-Y	0.62	437
V(CBA)-Y	0.70	389
V(NBA)-Y	0.68	420

formed using a BELSORP-mini instrument (Microtrac-BEL Corp.) at 77 K. The samples were purged with nitrogen for 2 h at 393 K before the measurements.

UV-vis spectra were measured using a V-650CA (JASCO Corp.) spectrometer to evaluate the band gap energy.

Fourier transform infrared (FTIR) spectra were recorded on a NICOLET 380 spectrometer using the KBr disk method to confirm the presence of ligands. Spectra were generated, collected 200 times and corrected for background noise.

The ligand elimination was monitored using a thermogravimetry-differential thermal analysis (TG-DTA) instrument (DTG-60, Shimadzu Corp.).

The V content of catalysts was measured on a Rigaku Primini X-ray fluorescence spectrometer.

The hydrogen peroxide content of the reaction solution was measured through potassium permanganate titration.

3. Results and Discussion

3. 1. Characterization of V Complexes Encapsulated in Y Zeolite Catalyst

3. 1. 1. Physical Properties of V-loaded and V Complex-encapsulated Catalysts

V loading and the Brunauer–Emmett–Teller (BET) surface areas are listed in **Table 1**. V-Y showed the highest V loading and the largest decrease in surface area compared to that of the H-Y zeolite. The ion-exchange ratio of V-Y was 48 %, and almost all the ion-exchange sites were replaced by V, indicating that V covers the surface of the zeolite and blocks the pore entrance. This finding might be attributed to the large decrease in the surface area of V-Y. In the V-complex-encapsulated in the Y zeolite catalyst, a lower V loading and higher BET surface area compared to those of V-Y were observed. The pores in the Y zeolite have a pore diameter of 7.4 nm and a super cage with a diameter of 1.4 nm in the pore, indicating that the number of V complexes encapsulated in the pores was limited. Therefore, the non-complexed V and the V blocking the pores were removed by washing after complex formation, decreasing the V loading and increasing the BET surface area.

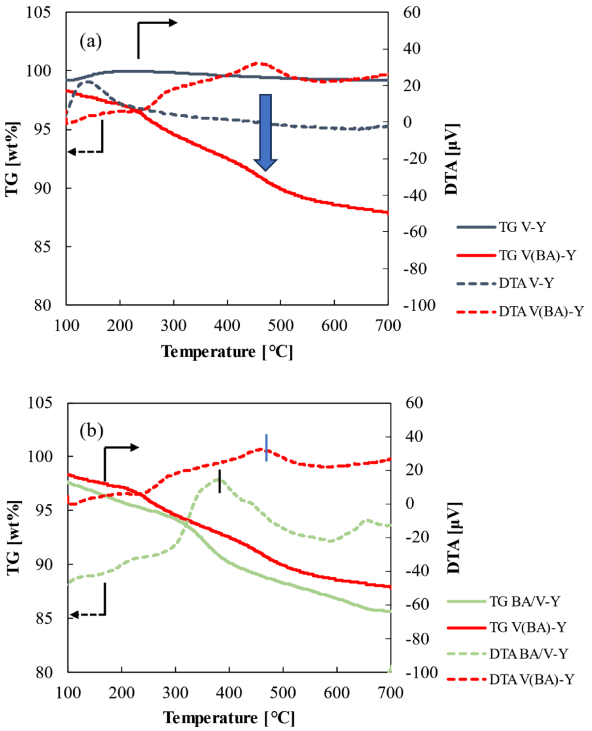

Fig. 1 TG-DTA Measurements of (a) V Ion-exchanged Catalyst (V-Y) and V Complexes Encapsulated in Y Zeolite Catalyst (V(BA)-Y), and (b) V(BA)-Y and a Catalyst with a Ligand Loaded on V-Y by the Impregnation Method (BA/V-Y)

3. 1. 2. TG-DTA

The difference in the TG-DTA behavior of the V-Y and V complex-encapsulated catalysts is shown in **Fig. 1(a)**. The weight-loss curve of the V-complex-encapsulated catalyst comprises three steps. The first step, at about 25-100 ℃, is due to the desorption of water from the catalyst. The second step, at 100-300 ℃, is the desorption of water adsorbed on the acid sites of the zeolite. The third step, above 300 ℃, is due to the elimination and the combustion of the ligand. The third peak was observed only for the V-complex-encapsulated catalyst. This finding indicates that a ligand was present in the V-complex-encapsulated catalyst. **Figure 1(b)** shows the TG-DTA results for BA/V-Y, a catalyst with a ligand loaded on V-Y by the impregnation method, and V(BA)-Y. In BA/V-Y, the exothermic peak derived from the combustion of the ligand was observed at about 400 ℃. Conversely, the peak was around 500 ℃ in V(BA)-Y. This peak shift was attributed to the ligand binding to V through complex formation, which makes the ligand more difficult to be desorbed from the catalyst than in the state where the ligand is dispersed on the carrier. Therefore, the exothermic peak of V(BA)-Y, corresponding to the burning of the ligands, shifted to a higher field owing to

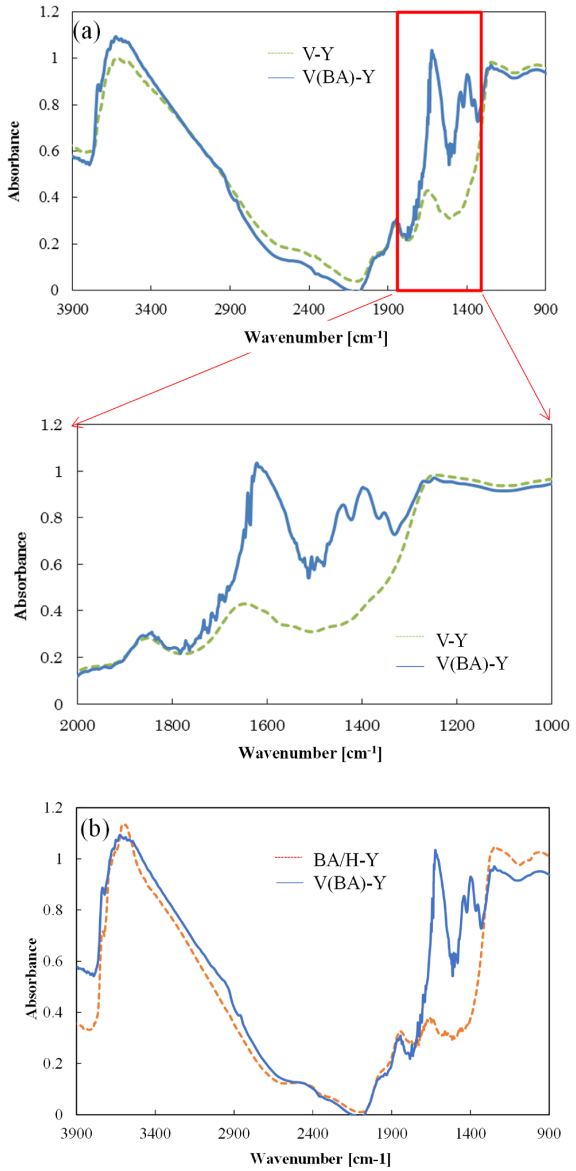

Fig. 2 Fourier Transform Infrared (FTIR) Spectra of (a) V Ion-exchanged Catalyst and V Complexes Encapsulated in Y Zeolite Catalyst (V(BA)-Y), and (b) V(BA)-Y and H-Y Zeolites Treated Using a Benzoic Solution (BA/H-Y)

the burning of the ligands.

3. 1. 3. FTIR Measurement

The FTIR spectra of V-Y and V(BA)-Y are shown in **Fig. 2(a)**. The V complex-encapsulated catalyst exhibited a peak at approximately 1600 cm^{-1}, which is assigned to aromatic C = C stretching[26], suggesting the presence of ligands in the catalyst. **Figure 2(b)** shows the FTIR spectra of V(BA)-Y and H-Y zeolites treated with a benzoic solution (BA/H-Y). This zeolite was obtained by stirring the H-Y zeolite in the ligand solution for 20 h, followed by filtration, washing, and drying. The FTIR spectra of V(BA)-Y and BA/H-Y showed no peak at approximately 1600 cm^{-1}. The ligand did not remain in the catalyst when V was absent. The peak derived from the ligand in the V-complex-encapsulated catalyst indicates that the ligand is coordinated with the V species in the catalyst.

3. 2. Evaluation of the Catalytic Activity of V-loaded and V Complex-encapsulated Catalysts

The results of the liquid-phase oxidation of benzene over the V-Y and V complex-encapsulated catalysts are shown in **Table 2**. Run 1 shows the phenol yield obtained using the fresh catalyst. In Run 2, the catalyst used in Run 1 was recycled, washed, and reused. The reusability of the V-loaded catalyst by the ion exchange method was extremely low because V, which works as the active species, was eluted into the reaction solution. By contrast, the V-complex-encapsulated catalyst exhibited improved reusability. Consequently, the V complexes were confined in the pores of the Y zeolite, preventing their elution into the reaction solution and prolonging the life of the catalyst.

Upon comparing the turnover number (TON) of each catalyst, it becomes evident that TON differs depending on the ligand of the complex, and the catalytic activity of the encapsulated catalyst was higher than that of the V-Y catalyst.

3. 3. Relationship between Hydrogen Peroxide Generation and Phenol Generation Activity

The catalytic activity of certain catalysts can be confirmed through hydrogen peroxide generation. Therefore, the yield of hydrogen peroxide produced during

Table 2 Phenol Production Activity Catalyzed Using Various V Catalysts

Catalyst	V content [mmol/g-cat.]	Yield of phenol [mmol/g-cat]		TON	Reusability [%]
		Run 1	Run 2[a)]		
V-Y	0.89	2.25	0.29	2.5	13
V(ABA)-Y	0.59	3.45	2.76	5.8	80
V(HBA)-Y	0.70	1.78	1.12	2.5	63
V(MBA)-Y	0.57	3.04	2.35	5.3	77
V(BA)-Y	0.68	1.44	0.89	2.1	62
V(CBA)-Y	0.62	2.15	1.65	3.5	77
V(NBA)-Y	0.59	3.45	2.76	5.8	80

a) Run 2 shows phenol formation activity over the reused catalyst.

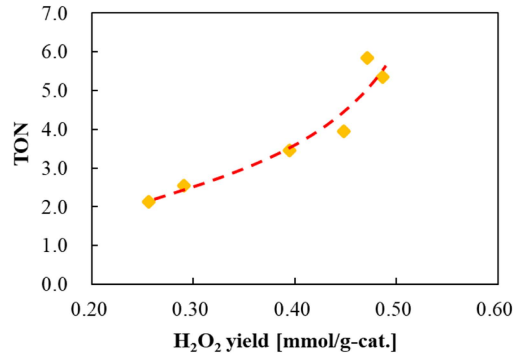

Fig. 3 Relationship between Hydrogen Peroxide Formation Yield and Energy Gap between V^{3+} and V^{4+} Complexes

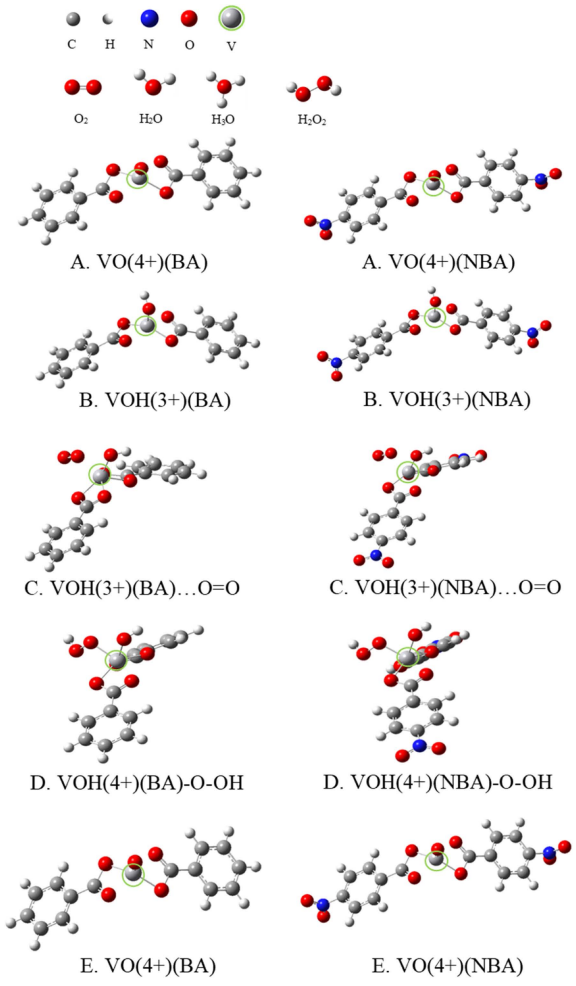

Fig. 4 Structures of V(BA) and V(NBA) in Each Reaction Stage

the reaction of the V-complex-encapsulated catalysts with different ligands was investigated, as shown in **Fig. 3**. In the reaction to produce phenol, hydrogen peroxide is formed as a reaction intermediate. The amount of hydrogen peroxide generated is directly related to phenol-forming activity. Thus, the generation of hydrogen peroxide appears to be the rate-determining step in this reaction.

Table 3 Formation Enthalpy of Vanadium Complexes by DFT Calculations

V complex	Energy gaps [a] [kcal/mol]				
	A	B	C	D	E
V(BA)	0	+29.7	+23.7	+32.8	+21.3
V(NBA)	0	+26.1	+24.1	+33.4	+21.3

a) Energy gaps of formation enthalpy between state A and B-E in Fig. 4.

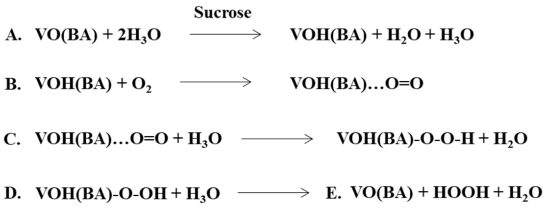

Scheme 1 Reaction Steps of Hydrogen Peroxide Formation Reaction over V Complex

3. 4. Examination of Hydrogen Peroxide Generation Process Using DFT Calculation

The rate-limiting step of phenol formation was studied by calculating the energy diagram of the process of producing hydrogen peroxide. The role of the V complex in the assumed reaction process was confirmed using DFT calculations, and the formation enthalpy of the structure was obtained. **Figure 4** shows the structures of the complexes, and the energy gaps based on initial stage A of the reaction are summarized in **Table 3**. A-E in **Table 3** correspond to A-E in **Scheme 1** and **Fig. 4**. The formation enthalpy of A was set to zero, and the difference in the enthalpy of B-E was calculated. Structure A indicates the minimum enthalpy of formation in A-E. In **Scheme 1**, the energy gap between stages A and B was the largest, suggesting that the reduction of the V complex, the reaction from stage A to stage B, has the largest energy barrier. Additionally, the ease of progress of the reduction reaction of the V complex from stage A to stage B significantly affected hydrogen peroxide production. Therefore, it was presumed that the factor that leads to different catalytic activities among the V complex catalysts with different ligands is the size of the energy barrier for the reduction of each V complex. Therefore, the energy gap for reducing the V complex with different ligands was calculated and compared with the respective hydrogen peroxide-producing activities.

Table 3 shows the calculation results for the energy barrier of the reduction of the V complex. **Figure 5** shows the energy gap between V^{3+} and V^{4+} and the amount of hydrogen peroxide generated. As shown in **Fig. 5**, a strong correlation was observed between the

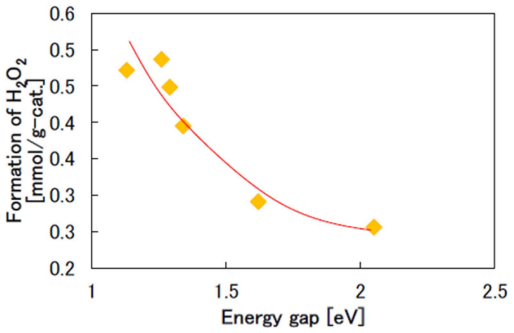

Fig. 5 Relationship between Hydrogen Peroxide Formation Yield and Energy Gaps between V^{3+} and V^{4+} Complexes Using DFT Calculations

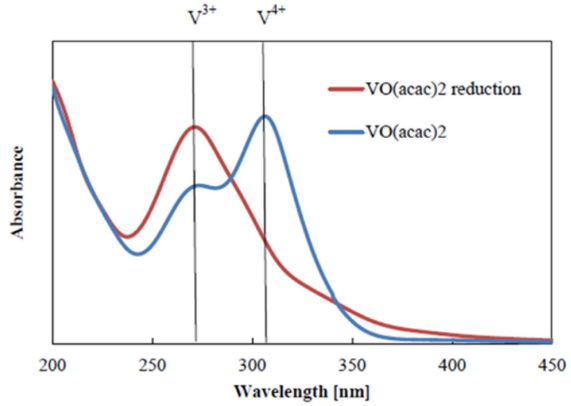

Fig. 6 UV-vis Spectrum of $VO(acac)_2$ Solution before and after Reaction with Sucrose

amount of hydrogen peroxide produced and the energy barrier during the reduction of the V complex. This finding suggests that the reduction of the V complex was the rate-limiting step in hydrogen peroxide generation. The stability of stage B of the V complex varied according to the ligand species, and the energy barrier changed simultaneously.

3. 5. Reduction Process of V Complex

The change in the valence of the V species in the reaction solution was examined using UV-vis measurements to confirm that the V species were reduced during the reaction. The vanadyl acetylacetonate complex ($VO(acac)_2$) was used as the model complex instead of $VO(BA)_2$. $VO(acac)_2$ solution was reacted with sucrose under reaction conditions without benzene, the reactant and the solution before and after the reaction were analyzed using UV-vis spectroscopy, and the reduction of the V species by sucrose was observed. The results are shown in **Fig. 6**. In the UV-vis spectrum of the $VO(acac)_2$ solution before the reduction reaction, a peak was observed at 308 nm, which was attributed to the V^{4+} d-d transition absorption of $VO(acac)_2$. In the UV-vis spectrum of the $VO(acac)_2$ solution after the reduction reaction, the peak at 308 nm decreased, and the peak at 270 nm increased. The peak at 270 nm was assigned to V^{3+} species, indicating that V^{4+} was reduced to V^{3+}. This result confirms the reduction of the V species.

In the presence of hydrogen peroxide, the oxidation of V^{4+} to V^{5+} was observed in the V complex with two molecules of quinaldic acid as ligands ($VO(QA)_2$) (see Fig. S1). V^{5+} oxidized by hydrogen peroxide was also shown to be re-reduced to V^{4+} in the presence of sucrose (see Fig. S2). These results suggest that the V species in the complex are reduced by sucrose and oxidized by the produced hydrogen peroxide as an intermediate in the reaction process.

3. 6. Possible Pathways of Benzene to Phenol Conversion

We explored two possible pathways for converting benzene to phenol, as shown in **Scheme 2**. Considering that the activity of peroxy acid is high because of its –OOH structure, peroxy acid (V–OOH) was utilized in the benzene oxidation reaction; the mechanism is shown in path A. Meanwhile, we assumed that hydrogen peroxide is produced by the decomposition of V–OOH and then subsequently reacts with benzene. This alternate path is denoted as path B.

3. 6. 1. Phenol Production via the Reaction between Benzene and the Intermediate V–OOH Structure (path A)

The intermediate with a V–OOH structure can be considered to be generated with protons during the oxygen activation process. Because the V–OOH structure is a type of peroxidic acid, it may have a high reaction activity. Here, we studied the reaction pathway between benzene and an intermediate with a V–OOH structure. The energy diagram for path A is shown in **Fig. 7**. DFT calculations showed that the O in the V–OOH structure is inserted into the C–H bond of benzene, and protons migrate toward O, producing phenol.

During this process, 330 kJ/mol of energy is required for inserting O, and 52 kJ/mol of energy is required to move protons. This enormous energy barrier renders path A unsuitable and impractical for this reaction.

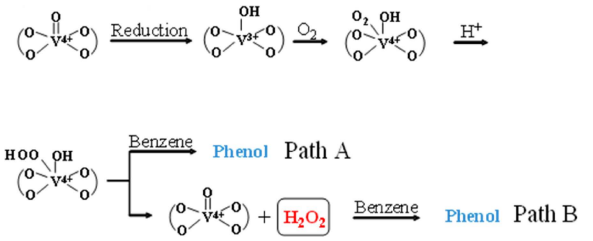

Scheme 2 Proposed Mechanism Pathway on Benzene to Phenol Conversion Starting from V–OOH

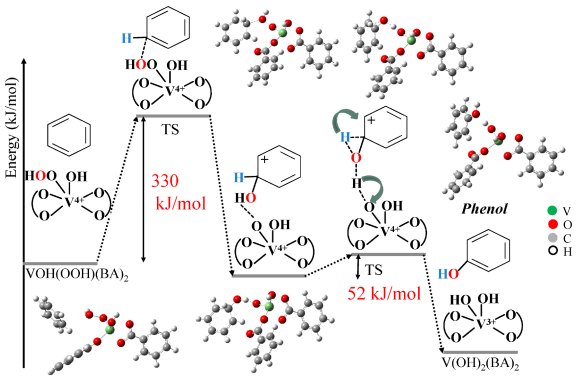

Fig. 7 Energy Diagram of Phenol Formation in Path A

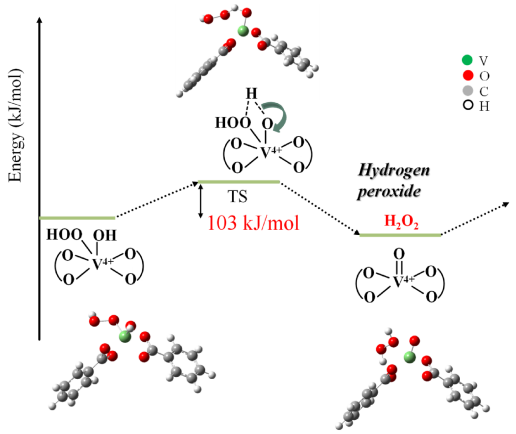

Fig. 8 Energy Diagram of Hydrogen Peroxide Formation Process in Path B

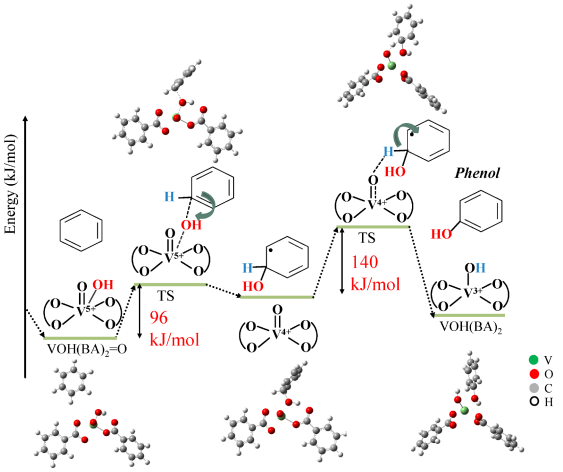

Fig. 9 Energy Diagram of Phenol Formation in Path B

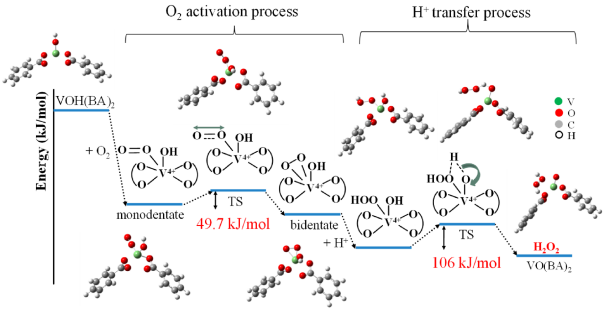

Fig. 10 Energy Diagram of Hydrogen Peroxide Formation Process in Path B in Water

3. 6. 2. Phenol Production via the Reaction between Hydrogen Peroxide and Benzene (path B)

The path of the production of hydrogen peroxide from the intermediate with V–OOH was studied. An energy diagram of this path is shown in **Fig. 8**. The protons, combined with V, migrate to –OOH to produce hydrogen peroxide, which is then separated from V. The activation energy for this process was 103 kJ/mol. Although the reaction between benzene and hydrogen peroxide was discussed, the mechanism for phenol production involving the movement of hydrogen peroxide molecules toward benzene remains unclear. Based on the detection of V^{5+} atoms in this experiment, a pathway for this reaction was explored when the V^{4+} catalyst was oxidized to the V^{5+} catalyst by hydrogen peroxide.

An energy diagram of the phenol production path, catalyzed by the V^{5+} catalyst derived from the reaction with hydrogen peroxide, is shown in **Fig. 9**. Benzene reaches the V^{5+} catalyst, and –OH reacts with benzene as an electrophilic catalyst, forming carbon radicals. The H atoms were separated from the C–H bonds in benzene under the effect of the catalyst, forming phenol. The activation energy for –OH to bond to benzene is 96 kJ/mol, and the separation of H requires 140 kJ/mol. Path B requires only 140 kJ/mol of energy, which is lower than that of path A. Therefore, the phenol production reaction followed path B, where hydrogen peroxide forms and reacts with benzene on the pentavalent catalysts.

3. 7. Hydrogen Peroxide Formation Pathway

The energy diagram for the solvent conditions is shown in **Fig. 10**. Even under solvent conditions, there was no significant change in the direction of the reaction or the structure of the intermediate. However, solvents substantially influence the reactants and products, leading to a lower activation energy than vacant conditions. The activation process of O_2 and the movement of H_2 forms hydrogen peroxide, with activation energies measuring 49.7 kJ/mol and 106 kJ/mol, respectively.

3. 8. The Calculation of the Pathway of Phenol Formation

Path B was more feasible than path A in a vacuum. Therefore, path B was placed in a solvent, and the activation energy was calculated under conditions similar

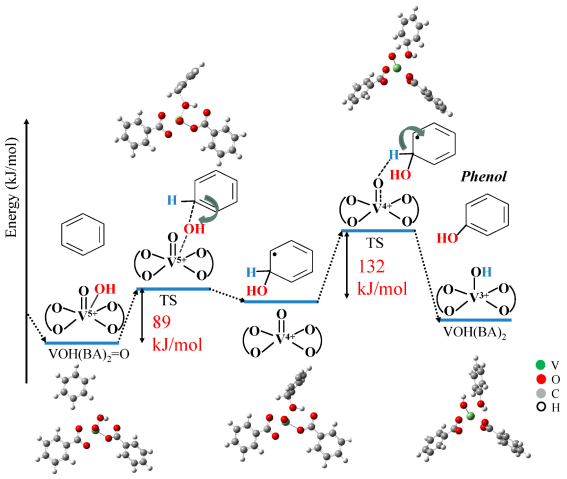

Fig. 11 Energy Diagram of Phenol Formation in Path B in Water

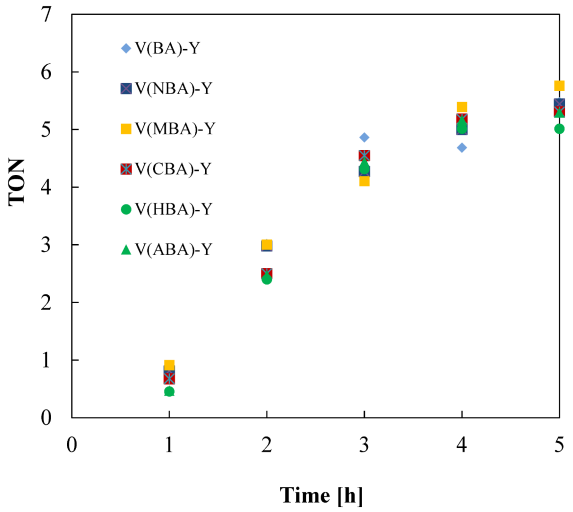

Fig. 12 Phenol Formation Activity of Various V Complexes Catalysts Using Hydrogen Peroxide as an Oxidant

to those of a real reaction. **Figure 11** shows an energy diagram of the phenol formation pathway when path B occurs in water. Benzene reaches the V^{5+} catalyst, and ⁻OH reacts with benzene as an electrophilic catalyst, forming carbon radicals.

The H atoms were separated from the C–H bonds in benzene under the effect of the catalyst, forming phenol. The activation energies for ⁻OH to bond to benzene are 89 kJ/mol and 132 kJ/mol to separate H. Because only 140 kJ/mol of energy is needed for path B, there is no notable difference between the vacuum and solvent conditions. It is believed that the reaction proceeds by changing the valence of V, and the overall charge is regarded as 0; thus, ideal data can be obtained even without solvent conditions.

3. 9. Phenol Formation Reaction with Hydrogen Peroxide

Subsequently, the influence of the ligand of the V complex on the hydrogen peroxide oxidation of benzene after the generation of hydrogen peroxide was examined. The oxidation reaction of benzene was performed using hydrogen peroxide as an oxidizing agent. The results are shown in **Fig. 12**. No difference was observed in the phenol yield with any of the V-complex-encapsulated catalysts, indicating that the oxidation of benzene with hydrogen peroxide occurs rapidly, with the ligand of the V-complex exerting minimal influence on this process.

Therefore, the catalytic activity varies depending on the type of ligand of the V complex because the ease of the redox progress of the V complex varies depending on the complex. This step was identified as the rate-limiting step in the present reaction.

4. Conclusions

Various characterization results suggested that the V complex was formed within the cage of the Y-type zeolite. Furthermore, it was confirmed that catalyst reusability significantly improved in a liquid-phase phenol synthesis reaction compared to the conventional impregnation method of V loading. In addition, catalytic activity differed depending on the type of complex; the smaller the energy gap between V^{3+} and V^{4+}, the higher the phenol-forming activity. This energy gap was related to hydrogen peroxide production, a reaction intermediate. Thus, the reaction mechanism of the present reaction was determined based on the rate of hydrogen peroxide generation. Finally, DFT calculations revealed the mechanism of liquid-phase benzene oxidation with the V-complex-encapsulated Y zeolite.

Supporting Information

Supplementary data associated with this article can be found in the online version at https://jstage.jst.go.jp/browse/jpi/-char/en (DOI: doi.org/10.1627/jpi.67.80).

References

1) Crabtree, R. H., *J. Chem. Soc. Dalton Trans.*, **17**, 2437 (2001).
2) Corma, A., Esteve, P., Martínez, A., *J. Catal.*, **161**, 11 (1996).
3) Parmeggiani, C., Cardona, F., *Green Chem.*, **14**, 547 (2012).
4) Ahmad, J. U., Räisänen, M. T., Leskelä, M., Repo, T., *Appl. Catal. A: General*, **180**, 411 (2012).
5) Fernandez, I., Khiar, N., *Chem. Rev.*, **103**, (9), 3651 (2003).
6) Ichihashi, Y., Kamizaki, Y., Terai, N., Taniya, K., Tsuruya, S., Nishiyama, S., *Catal. Lett.*, **134**, 324 (2010).
7) Panov, G. I., Sheveleva, G. A., Kharitonov, A. S., Romannikov, V. N., *Appl. Catal. A: General*, **82**, 31 (1992).
8) Chernyavsky, V. S., Pirutko, L. V., Uriarte, A. K., Kharitonov, A. S., Panov, G. I., *J. Catal.*, **245**, (2), 466 (2007).
9) Yoo, J. S., Sohail, A. R., Grimmer, S. S., Shyu, J. Z., *Appl. Catal. A: General*, **117**, 1 (1994).
10) Jia, J., Pillai, K. S., Sachtler, W. M. H., *J. Catal.*, **221**, 119 (2004).
11) Horváth, B., Sustek, M., Skriniarová, J., Omastová, M., Dobrocka, E., Hronec, M., *Appl. Catal. A: General*, **481**, 71

(2014).
12) Yang, H., Chen, J., Li, J., Lv, Y., Gao, S., *Appl. Catal. A: General*, **415**, (16), 22 (2012).
13) Sumimoto, S., Tanaka, C., Yamaguchi, S., Ichihashi, Y., Nishiyama, S., Tsuruya, S., *Ind. Eng. Chem. Res.*, **45**, 7444 (2006).
14) Nomiya, K., Yanagibayashi, H., Nozaki, C., Kondoh, K., Hiramatsu, E., Shimizu, Y., *J. Mol. Catal. A Chem.*, **114**, (1), 181 (1996).
15) Stöckmann, M., Konietzni, F., Notheis, J. U., Voss, J., Keune, W., Maier, W. F., *Appl. Catal. A: General*, **208**, (1), 343 (2001).
16) Parida, K. M., Rath, D., *Appl. Catal. A: General*, **321**, (2), 101 (2007).
17) Liu, Y., Murata, K., Inaba, M., *Catal. Commun.*, **6**, (10), 679 (2005).
18) Bui, T. D., Kimura, A., Ikeda, S., Matsumura, M., *J. Am. Chem. Soc.*, **132**, (24), 8453 (2010).
19) Seo, Y., Mukai, Y., Tagawa, T., Goto, S., *J. Mol. Catal. A Chem.*, **120**, (1), 149 (1997).
20) Miyake, T., Hamada, M., Niwa, H., Nishizuka, M., Oguri, M., *J. Mol. Catal. A Chem.*, **178**, (1-2), 199 (2002).
21) Takata, K., Yamaguchi, S., Nishiyama, S., Tsuruya, S., *J. Mol. Catal. A Chem.*, **225**, 125 (2005).
22) Miyahara, T., Kanzaki, H., Hamada, R., Kuroiwa, S., Nishiyama, S., Tsuruya, S., *J. Mol. Catal. A Chem.*, **176**, 141 (2001).
23) Okemoto, A., Inoue, Y., Ikeda, K., Tanaka, C., Taniya, K., Ichihashi, Y., Nishiyama, S., *Chem. Lett.*, **43**, 1734 (2014).
24) Masumoto, Y., Hamada, R., Yokota, K., Nishiyama, S., Tsuruya, S., *J. Mol. Catal. A Chem.*, **184**, 215 (2002).
25) Yamaguchi, S., Sumimoto, S., Ichihashi, Y., Nishiyama, S., Tsuruya, S., *Ind. Eng. Chem.*, **44**, 1 (2005).
26) Mannar, R., Maurya, A. K., Chandrakar, S. C., *J. Mol. Catal. A: Chem.*, **278**, 12 (2007).

……

要　　旨

ベンゼンの液相酸化反応に用いる V 錯体内包触媒における配位子効果

谷　翔太郎[†1)]，市橋　祐一[†1),†2)]

[1)] 神戸大学大学院工学研究科応用化学専攻，657-8501 神戸市灘区六甲台町1-1

[2)] 神戸大学先端膜工学研究センター，657-8501 神戸市灘区六甲台町1-1

ship-in-a-bottle 法でバナジウム錯体を Y 型ゼオライトの細孔内に形成させたバナジウム錯体内包 Y 型ゼオライト触媒を用い，ベンゼンの液相酸化反応によるフェノール生成反応について検討を行った。結果，Y 型ゼオライトに含浸法でバナジウムを担持した触媒を用いた場合に観測されたバナジウム種の溶出はバナジウム錯体内包触媒では抑制され，ベンゼンの酸化反応が効率よく進行した。また，バナジウム錯体の配位子の影響について検討したところ，配位子の違いがフェノール生成活性に大きく影響を与えることが示唆された。密度汎関数理論（DFT）計算を用いて検討したところ，配位子の種類はバナジウムの3価と4価の間のエネルギーギャップに影響し，このエネルギーギャップが小さいものほどフェノール生成活性が高いことが明らかとなった。

……